

Power law persistence in the atmosphere: An ideal test bed for climate models

Armin Bunde^a, Jan Eichner^a, Rathinaswamy Govindan^{a,b}, Shlomo Havlin^b, Eva Koscielny-Bunde^{a,c}, Diego Rybski^{a,b} and Dmitry Vjushin^b

^a*Institut für Theoretische Physik III, Universität Giessen, D-35392 Giessen, Germany*

^b*Minerva Center and Department of Physics, Bar Ilan University, Israel*

^c*Potsdam Institute for Climate Research, D-14412 Potsdam, Germany*

Abstract

We review recent results on the appearance of long-term persistence in climatic records and how they can be used to evaluate climate models. The persistence can be characterized, for example, by the correlation $C(s)$ of temperature variations separated by s days. We show that, contrary to previous expectations, $C(s)$ decays for large s as a power law, $C(s) \sim s^{-\gamma}$. For continental stations, the exponent γ is always close to 0.7, while for stations on islands $\gamma \cong 0.4$. In contrast to the temperature fluctuations, the fluctuations of the rainfall usually cannot be characterized by long term power law correlations but rather by pronounced short term correlations. The universal persistence law for the temperature fluctuations on continental stations represents an ideal (and uncomfortable) test bed for the state of the art global climate models and allows to evaluate their performance.

1. Introduction

The persistence of weather states on short terms is a well-known phenomenon: A warm day is more likely to be followed by a warm day than by a cold day and vice versa. The trivial forecast that the weather of tomorrow is the same as the weather of today was, in previous times, often used as a "minimum skill" forecast for assessing the usefulness of short term weather forecasts. The typical time scale for weather changes is about one week, a time period which corresponds to the average duration of so-called "general weather regimes" or "Grosswetterlagen", so this type of short-term persistence usually stops after about one week. On larger scales, other types of persistence occur, one of them is related to circulation patterns associated with blocking [4]. A blocking situation occurs when a very stable high pressure system is established over a particular region and remains in place for several weeks. As a result the weather in the region of the high remains fairly persistent throughout this period. Furthermore, transient low pressure systems are deflected around the blocking high so that the region downstream of the high experiences a larger than usual number of storms. On even longer terms, a source for weather persistence might be slowly varying external (boundary) forcing such as sea surface temperatures and anomaly patterns. On the scale of months to seasons, one of the most pronounced phenomenon is the El Nino Southern Oscillation (ENSO) event which occurs every 3-5 years and which strongly affects the weather over the tropical Pacific as well as over North America [16].

The question is, *how* the persistence that might be generated by very different mechanisms on different time scales, decays with time s . The answer to this question is not easy. Correlations, and in particular long term correlations, can be masked by trends that are generated, e.g., by the well known urban warming. Even uncorrelated data in

the presence of long-term trends may look like correlated ones, and, on the other hand, long-term correlated data may look like uncorrelated data influenced by a trend.

Therefore, in order to distinguish between trends and correlations one needs methods that can systematically eliminate trends. Those methods are available now: both wavelet techniques (WT) (see e. g. [1]) and detrended fluctuation analysis (DFA) (see, e. g. [15, 3]) can systematically eliminate trends in the data and thus reveal intrinsic dynamical properties such as distributions, scaling and long-range correlations very often masked by nonstationarities.

In recent studies [11, 5, 17] we have used DFA and WT to study temperature and precipitation correlations in different climatic zones on the globe. The results indicate that the temperature variations are long range power law correlated above some crossover time that is of the order of 10 days. Above 10d, the persistence, characterized by the auto-correlation $C(s)$ of temperature variations separated by s days, decays as

$$C(s) \sim s^{-\gamma}, \quad (1)$$

where, most interestingly, the exponent γ has roughly the same value $\gamma \cong 0.7$ for all continental records. For small islands the correlations are more pronounced, with γ around 0.4. This value is close to the value obtained recently for correlations of sea-surface temperatures [12]. In marked contrast, for most stations the precipitation records do not show indications of long range temporal correlations on scales above 6 months. Our results are supported by independent analysis by several groups [13, 14, 18].

The fact that the correlation exponent varies only very little for the continental atmospheric temperatures, presents an ideal test bed for the performance of the global climate models, as we will show below. We present an analysis of the two standard scenarios (greenhouse gas forcing only and greenhouse gas plus aerosols forcing) together with the analysis of a control run. Our analysis points to clear deficiencies of the models. For further discussions we refer to [7].

The article is organized as follows: In Section 2, we describe one of the detrending analysis methods, the detrended fluctuation analysis (DFA). In Section 3, we review the application of this method to both atmospheric temperature and precipitation records. In Section 4, finally, we describe how the "universal" persistence law for the atmospheric temperature fluctuations on continental stations can be used to test the three scenarios of the state-of-the-art climate models.

2. The methods of analysis

Consider, e.g., a record T_i , where the index i counts the days in the record, $i = 1, 2, \dots, N$. The T_i may represent the maximum daily temperature or the daily amount of precipitation, measured at a certain meteorological station. For eliminating the periodic seasonal trends, we concentrate on the departures of the T_i , $\Delta T_i = T_i - \bar{T}_i$, from their mean daily value \bar{T}_i for each calendar date i , say 1st of April, which has been obtained by averaging over all years in the record.

Quantitatively, correlations between two ΔT_i values separated by n days are defined by the (auto) correlation function

$$C(n) \equiv \langle \Delta T_i \Delta T_{i+n} \rangle = \frac{1}{N-n} \sum_{i=1}^{N-n} \Delta T_i \Delta T_{i+n}. \quad (2)$$

If the ΔT_i are uncorrelated, $C(n)$ is zero for n positive. If correlations exist up to a certain number of days n_\times , the correlation function will be positive up to n_\times and vanish above n_\times . A direct calculation of $C(n)$ is hindered by the level of noise present in the finite records, and by possible nonstationarities in the data.

To reduce the noise we do not calculate $C(n)$ directly, but instead study the “profile”

$$Y_m = \sum_{i=1}^m \Delta T_i. \quad (3)$$

We can consider the profile Y_m as the position of a random walker on a linear chain after m steps. The random walker starts at the origin and performs, in the i th step, a jump of length ΔT_i to the right, if ΔT_i is positive, and to the left, if ΔT_i is negative. The fluctuations $F^2(s)$ of the profile, in a given time window of size s , are related to the correlation function $C(s)$. For the relevant case (1) of long-range power-law correlations, $C(s) \sim s^{-\gamma}$, $0 < \gamma < 1$, the mean-square fluctuations $\overline{F^2(s)}$, obtained by averaging over many time windows of size s (see below) asymptotically increase by a power law [2],

$$\overline{F^2(s)} \sim s^{2\alpha}, \quad \alpha = 1 - \gamma/2. \quad (3)$$

For uncorrelated data (as well as for correlations decaying faster than $1/s$), we have $\alpha = 1/2$.

For the analysis of the fluctuations, we employ a hierarchy of methods that differ in the way the fluctuations are measured and possible trends are eliminated (for a detailed description of the methods we refer to [10]).

(i) In the simplest type of fluctuation analysis (FA) (where trends are not going to be eliminated), we determine the difference of the profile at both ends of each window. The square of this difference represents the square of the fluctuations in each window.

(ii) In the *first order* detrended fluctuation analysis (DFA1), we determine in each window the best linear fit of the profile. The variance of the profile from this straight line represents the square of the fluctuations in each window.

(iii) In general, in the n -th order DFA (DFA n) we determine in each window the best n -th order polynomial fit of the profile. The variance of the profile from these best n -th order polynomials represents the square of the fluctuations in each window.

By definition, FA does not eliminate trends similar to the Hurst method and the conventional power spectral methods [6]. In contrast, DFA n eliminates trends of order n in the profile and $n-1$ in the original time series. Thus, from the comparison of fluctuation functions $F(s)$ obtained from different methods one can learn about long term correlations and types of trends, which cannot be achieved by the conventional techniques.

3 Analysis of temperature and precipitation records

Figure 1 shows the results of the FA and DFA analysis of the maximum daily temperatures T_i of the following weather stations (the length of the records is written within the parentheses): (a) Cheyenne (USA, 123 y), (b) Edinburgh (UK, 102 y), (c) Campbell Island (New Zealand, 57 y), and (d) Sonnblick (Austria, 108 y). The results are typical for a large number of records that we have analyzed so far (see [11, 5]). Cheyenne has continental climate, Edinburgh is on coastlines, Campbell Island is a small island in the Pacific ocean, and the weather station of Sonnblick is on top of a mountain.

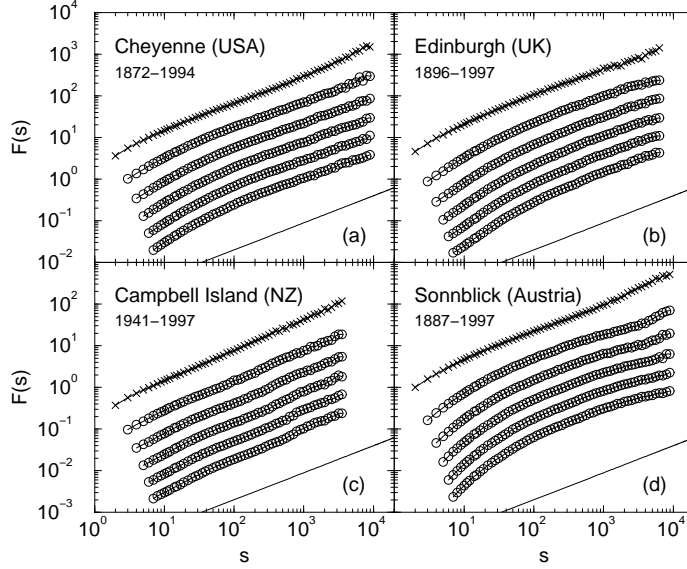


Figure 1: Analysis of daily temperature records of 4 representative weather stations. The 4 figures show the fluctuation functions obtained by FA, DFA1, DFA2, DFA3, DFA4, and DFA5 (from top to bottom) for the 4 sets of data. The scale of the fluctuation functions is arbitrary. In each panel, a line with slope 0.65 is shown as guide to the eye.

In the log-log plots, all curves are (except at small s -values) approximately straight lines. For both the stations inside the continents and along coast lines the slope is $\alpha \cong 0.65$. There exists a natural crossover (above the DFA-crossover) that can be best estimated from FA and DFA1. As can be verified easily, the crossover occurs roughly at $t_c = 10d$, which is the order of magnitude for a typical Grosswetterlage. Above t_c , there exists long-range persistence expressed by the power-law decay of the correlation function with an exponent $\gamma = 2 - 2\alpha \cong 0.7$. These results are representative for the large number of records we have analyzed. They indicate that the exponent is "universal", i.e. does not depend on the location and the climatic zone of the weather station. Below t_c , the fluctuation functions do not show universal behavior and reflect the different climatic zones.

However, there are exceptions from the universal behavior, and these occur for locations on small islands and on top of large mountains. In the first case, the exponent can be considerably larger, $\alpha \cong 0.8$, corresponding to $\gamma \cong 0.4$. In the second case, on top of a mountain, the exponent can be smaller, $\alpha \cong 0.58$, corresponding to $\gamma \cong 0.84$.

Next we consider precipitation records. Figure 2 shows the results of the FA and DFA analysis of the daily precipitation P_i of the following weather stations (the length of the records is written within the parentheses): Cheyenne (USA, 117 y) Fig. 2a, Edinburgh (UK, 102 y) Fig. 2b, Campbell Island (New Zealand, 57 y) Fig. 2c and Sonnblick (Austria, 108 y) Fig. 2d. The results are typical and represent a large number of records that we have analyzed so far (see [17]).

In the log-log plots, all curves are (except at small s -values) approximately straight lines at large times, with a slope close to 0.5. If there exist long range correlations, then they are very small. Some exceptions are again stations on top of a mountain, where the exponent might be around 0.6, but this happens only very rarely. In most cases, the exponent is between 0.5 and 0.55, pointing to uncorrelated or weakly correlated behavior

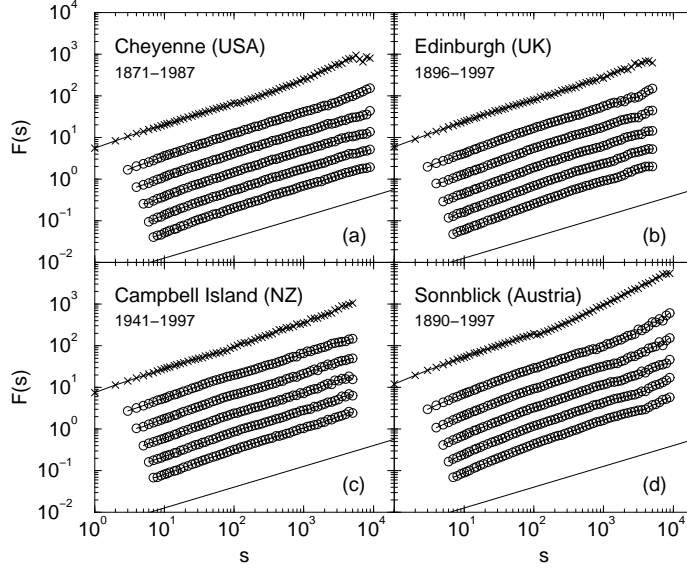


Figure 2: Analysis of daily precipitation records of 4 representative weather stations. The 4 figures show the fluctuation functions obtained by FA, DFA1, DFA2, DFA3, DFA4, and DFA5 (from top to bottom) for the 4 sets of data. The scale of the fluctuation functions is arbitrary. In each panel, a line with slope 0.5 is shown as guide to the eye.

at large time spans. Unlike to the temperature records, the exponents actually do not depend on specific climatic or geographic conditions.

Figure 3 summarizes the results for exponents α for (a) temperature records and (b) precipitation records. Different climatological conditions are marked in the histograms. First we concentrate on the temperature records (Fig. 3a). One can see clearly that for continental and coastline stations, the average exponent is close 0.65, with a variance of 0.03. For the islands (where only few records are available) the average value of α is 0.78, with quite a large variance of 0.08. The variance is large, since stations on larger islands, like Wrangelija, behave more like continental stations, with an exponent close to 0.65. For the precipitation records (Fig. 3b), the average exponent α is close to 0.54, with a variance close to 0.05, and does not depend significantly on the climatic conditions around a weather station.

Since for the temperature records the exponent for continental and coastline stations does not depend on the location of the meteorological station and its local environment, the power law behavior can serve as an ideal test for climate models where regional details cannot be incorporated and therefore regional phenomena like urban warming cannot be accounted for. The power law behavior seems to be a global phenomenon and therefore should also show up in the simulated data of the global climate models (GCM).

4 Test of global climate models

The state of the art climate models that are used to estimate future climate are coupled atmosphere-ocean general circulation models (AOGCMs) [19, 8]. The models provide numerical solutions of the Navier Stokes equations devised for simulating meso-scale to large-scale atmospheric and oceanic dynamics. In addition to the explicitly resolved scales

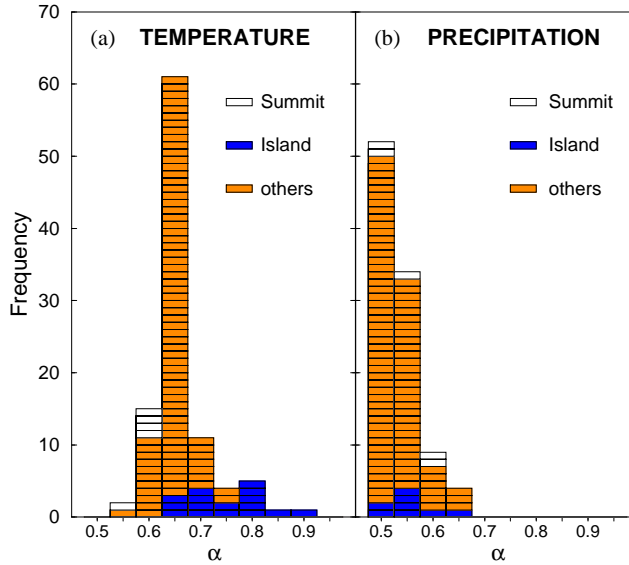


Figure 3: Histogram of the values of the fluctuation exponents α (a) for daily temperature records and (b) for daily precipitation records.

of motions, the models also contain parameterization schemes representing the so-called subgrid-scale processes, such as radiative transfer, turbulent mixing, boundary layer processes, cumulus convection, precipitation, and gravity wave drag. A radiative transfer scheme, for example, is necessary for simulating the role of various greenhouse gases such as CO_2 and the effect of aerosol particles. The differences among the models usually lie in the selection of the numerical methods employed, the choice of the spatial resolution [20], and the subgrid-scale parameters.

Three scenarios have been studied by the models, and the results are available, for 4 models, from the IPCC Data Distribution Center [21]. The first scenario represents a control run where the CO_2 content is kept fixed. In the second scenario, one considers only the effect of greenhouse gas forcing (GHG). The amount of greenhouse gases is taken from the observations until 1990 and then increased at a rate of 1% per year. In the third scenario, also the effect of aerosols (mainly sulphates) in the atmosphere is taken into account. Only direct sulphate forcing is considered; until 1990, the sulphate concentrations are taken from historical measurements, and are increased linearly afterwards. The effect of sulphates is to mitigate and partially offset the greenhouse gas warming. Although this scenario represents an important step towards comprehensive climate simulation, it introduces new uncertainties - regarding the distributions of natural and anthropogenic aerosols and, in particular, regarding indirect effects on the radiation balance through cloud cover modification etc. [9].

For the test, we consider the monthly temperature records from those four AOGCMs where the three scenarios data are available from the Internet: CSIRO-Mk2 (Melbourne), CCSR/NIES (Tokyo), ECHAM4/OPYC3 (Hamburg), and CGCM1 (Victoria, Canada). We extracted the data for six representative sites around the globe (Prague, Kasan, Seoul, Luling (Texas), Vancouver, and Melbourne). For each model and each of the three scenarios, we selected the temperature records of the 4 grid points closest to each site, and bilinearly interpolated the data to the location of the site. Figure 4 shows representative results of the fluctuation functions, calculated using DFA3, for two sites (Kasan (Russia)

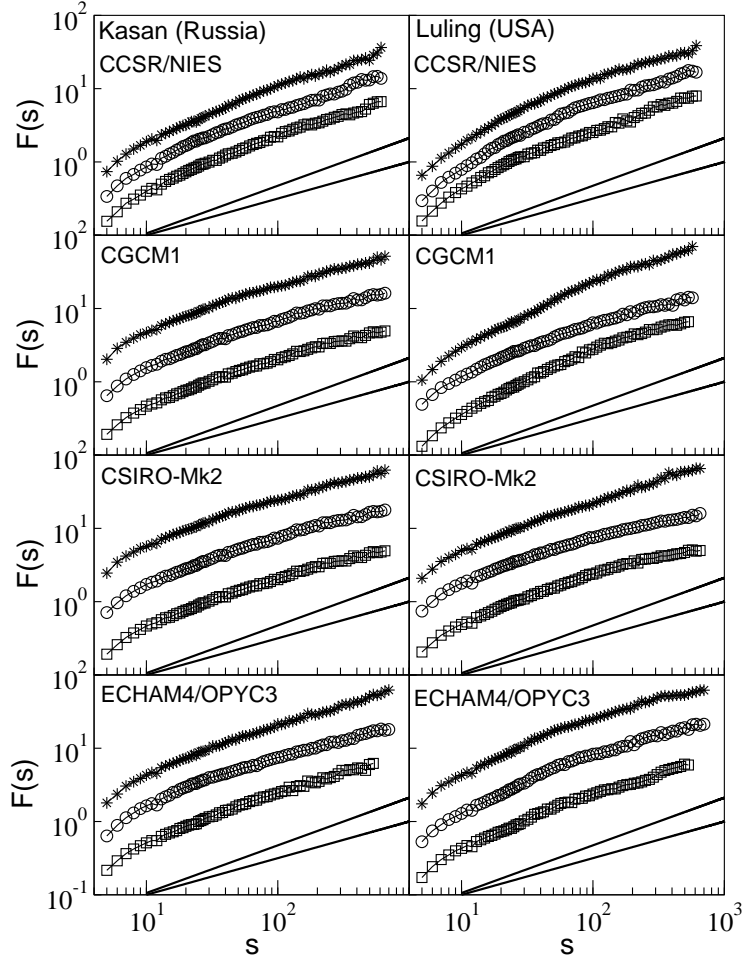


Figure 4: Comparison of the scaling performance of the three scenarios: control run (stars), greenhouse gas forcing only (circles) and greenhouse gas plus aerosols (boxes). All curves are obtained by applying DFA3 to the monthly mean of the daily maximum temperatures generated by the four AOGCMs. The lines with slopes 0.65 and 0.5 are shown as guide to the eye. For details of the records, we refer to [21].

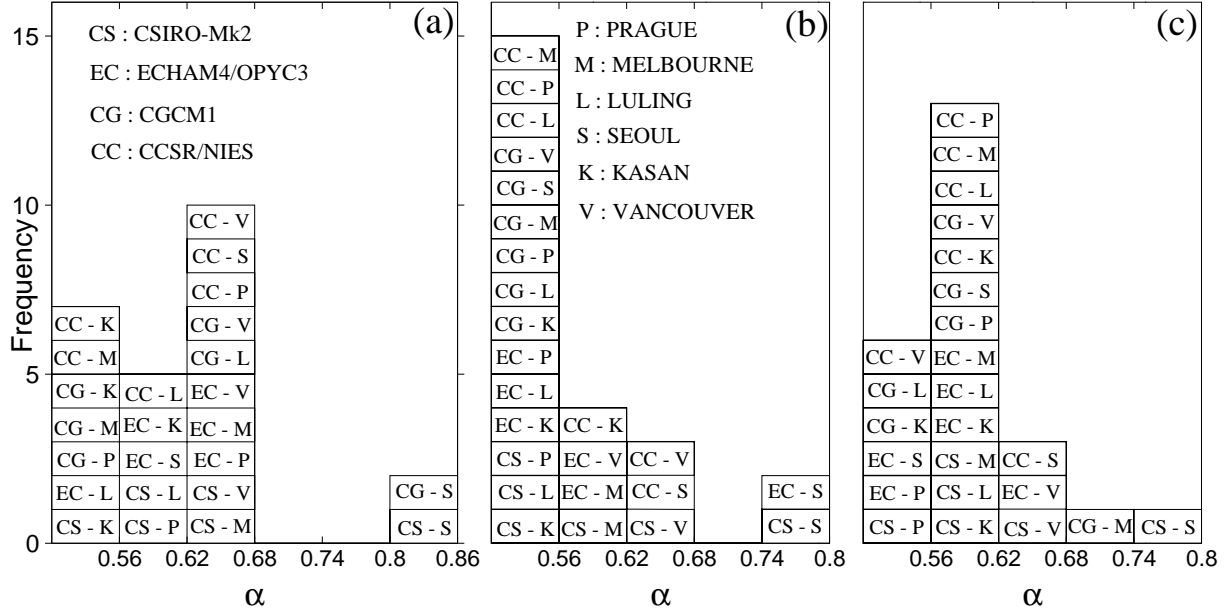


Figure 5: Histogram of the values of the fluctuation exponent (α) obtained from the simulations of the four AOGCMs (listed in (a)), for six sites (listed in (b)). The three panels are for the three scenarios: (a) control run, (b) greenhouse gas forcing only, and (c) greenhouse gas plus aerosol forcing. The entries in each box represent ‘Model - Site’.

and Luling (Texas)) for the 4 models and the three scenarios. As seen in Fig. 4 most of the DFA curves approach the slope of 0.5. However, the control runs seem to show a somewhat better performance, i.e., many of them have a slope close to 0.65 (e.g., Luling (CSIRO-Mk2)), and the greenhouse gas only scenario show the worst performance. The actual long term exponents α for the three scenarios of the 4 models for the 6 cities are summarized in Fig. 5(a-c). Each histogram consists of 24 blocks and every block is specified by the model and the city.

For the control run (Fig. 5a) there is a peak at $\alpha \cong 0.65$ but more than half of the exponents are below $\alpha \cong 0.62$. For the greenhouse gas only scenario (Fig. 5b), the histogram shows a pronounced maximum at $\alpha = 0.5$. For best performance, all models should have exponents α close to 0.65, corresponding to a peak of height 24 in the window between 0.62 and 0.68. Actually more than half of the exponents are close to 0.5, while only 3 exponents are in the proper window between 0.62 and 0.68. Figure 5c shows the histogram for the greenhouse gas plus aerosol scenario, where in addition to the greenhouse gas forcing, also the effects of aerosols are taken into account. For this case, there is a pronounced maximum in the α window between 0.56 and 0.62 (more than half of the exponents are in this window), while again only 3 exponents are in the proper range between 0.62 and 0.68. This shows that although the greenhouse gas plus aerosol scenario is also far from reproducing the scaling behavior of the real data, its overall performance is better than the performance of the greenhouse gas scenario. The best performance is observed for the control run, which points to remarkable deficiencies in the way the forcings are introduced into the models.

Acknowledgments

We are grateful to Prof. H.J. Schellnhuber and Prof. S. Brenner for very useful discussions. We like to acknowledge financial support by the Deutsche Forschungsgemeinschaft and the Israel Science Foundation.

References

- [1] Arneodo, A., dAubentonCarafa, Y., Bacry, E., Graves, P.V., Muzy, J.F., Thermes, C. "Wavelet based fractal analysis of DNA sequences". *Physica D* 96 (1996): 291-320.
- [2] Bunde, A., and Havlin, S. (eds.). *Fractals in Science*. New York: Springer, 1995.
- [3] Bunde, A., Havlin, S., Kantelhardt, J.W., Penzel, T., Peter, J.H., Voigt, K. "Correlated and uncorrelated regions in heart-rate fluctuations during sleep". *Phys. Rev. Lett.* 85 (2000): 3736-3739.
- [4] Charney, J.G., and Devore, J.G., *J. Atmos. Sci.* 36 (1979): 1205.
- [5] Eichner, J., Bunde, A., Havlin, S., Koscielny-Bunde, E., Schellnhuber, H.J. "Scaling and multiscaling of atmospheric temperature fluctuations: A detrended fluctuation analysis". Preprint (2002).
- [6] Feder, J. *Fractals*. New York: Plenum, 1989.
- [7] Govindan, R. B., Vjushin, D., Brenner, S., Bunde, A., Havlin S., H.-J. Schellnhuber H.-J. "Long-range correlations and trends in global climate models: Comparison with real data". *Physica A* 294 (2001): 239-; Vjushin, D., Govindan, R. B., Brenner, S., Bunde, A., Havlin, S., Schellnhuber, H.-J. "Lack of scaling in global climate models". *J. Phys. Cond. Mat.* 14 (2002): 2275; Govindan, R. B., Vjushin, D., Brenner, S., Bunde, A., Havlin, S., Schellnhuber, H.-J. "Global climate models violate scaling of the observed atmospheric variability". *Phys. Rev. Lett.*, (submitted) (2002).
- [8] Hasselmann, K. "Multi-pattern fingerprint method for detection and attribution of climate change", *Multi-fingerprint detection and attribution analysis of greenhouse gas, greenhouse gas-plus-aerosol and solar forced climate change. Climate Dynamics* 13 (1997): 601-634 and references there in.
- [9] Houghton, J.T. (editor). "Climate Change 2001: The Scientific Basis, Contribution of Working Group I to the Third Assessment Report of the Intergovernmental Panel on Climate Change (IPCC)". Cambridge: Cambridge University Press, 2001.
- [10] Kantelhardt, J. W., Koscielny-Bunde, E., Rego, H. A., Havlin, S., Bunde, A. "Detecting long-range correlations with detrended fluctuation analysis". *Physica A* 295 (2001): 441-454.
- [11] Koscielny-Bunde, E., Bunde, A., Havlin, S., Roman, H. E., Goldreich, Y., Schellnhuber, H.-J. "Indication of a universal persistence law governing atmospheric variability". *Phys. Rev. Lett.* 81 (1998): 729-732; Koscielny-Bunde, E., Bunde, A., Havlin, S., Goldreich, Y. "Analysis of daily temperature fluctuations". *Physica A* 231 (1996): 393-396.

- [12] Monetti, R. A., Havlin, S., and Bunde, A. "Long term persistence in the sea surface temperature fluctuations". Phys. Rev. Lett., (submitted) (2002).
- [13] Pelletier, J.D., Turcotte, D.L. "Long-range persistence in climatological and hydrological time series: analysis, modeling and application to drought hazard assessment". J. Hydrol. 203 (1997): 198-208.
- [14] Pelletier, J.D. "Analysis and modeling of the natural variability of climate". J. Climate 10 (1997): 1331-1342.
- [15] Peng, C.-K., Buldyrev, S. V., Havlin, S., Simons, M., Stanley, H. E. , Goldberger, A. L. "Mosaic Organization of DNA Nucleotides". Phys. Rev. E 49 (1994): 1685-1689.
- [16] Philander, S.G. "El Nino, La Nina and the Southern Oscillation". International Geophysics Series, Vol 46 (1990).
- [17] Rybski, D., Bunde, A., Havlin, S., Schellnhuber, H.J. "Detrended fluctuation analysis of precipitation records: Scaling and multiscaling". Preprint (2002).
- [18] Talkner, P., Weber, R.O. "Power spectrum and detrended fluctuation analysis: Application to daily temperatures". Phys. Rev. E 62 (2000): 150-160.
- [19] IPCC: "The Regional Impacts of Climate Change. An Assessment of Vulnerability". Cambridge: Cambridge University Press, 1998.
- [20] A typical climate module within the overall AOGCM machinery will have a grid spacing of 300-500 km and 10-20 vertical layers as compared to a weather forecasting model with a grid spacing of 100 km or less and 30-40 layers.
- [21] http://ipcc-ddc.cru.uea.ac.uk/dkrz/dkrz_index.html